

**Flanders**  
State of  
the Art

15\_026\_1  
FHR reports

## Wave climate for inland vessels between Zeebrugge and the mouth of the Western Scheldt

Estimation by the Belgian coast model in SWAN

DEPARTMENT  
MOBILITY &  
PUBLIC  
WORKS

[www.flandershydraulicsresearch.be](http://www.flandershydraulicsresearch.be)



# **Wave climate for inland vessels between Zeebrugge and the mouth of the Western Scheldt**

Estimation by the Belgian coast model in SWAN

Suzuki, T.; Hassan, W.; Kolokythas, G.; Verwaest, T.; Mostaert, F

Oktober 2016

WL2016R15\_026\_1

This publication must be cited as follows:

Suzuki, T.; Hassan, W.; Kolokythas, G.; Verwaest, T.; Mostaert, F (2016). Wave climate for inland vessels between Zeebrugge and the mouth of the Western Scheldt: Estimation by the Belgian coast model in SWAN. Version 5.0. FHR Reports, 15\_026. Flanders Hydraulics Research: Antwerp, Belgium.






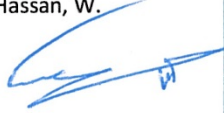


Nothing from this publication may be duplicated and/or published by means of print, photocopy, microfilm or otherwise, without the written consent of the publisher.

### Document identification

Title:	Wave climate for inland vessels between Zeebrugge and the mouth of the Western Scheldt: Estimation by the Belgian coast model in SWAN			
Customer:	Maritime Access Division	Ref.:	WL2016R15_026_1	
Keywords (3-5):	Golven; Binnenvaart; Zeebrugge; Knokke-Heist			
Text (p.):	30	Appendices (p.):	4	
Confidentiality:	<input type="checkbox"/> Yes	Exceptions:	<input type="checkbox"/> Customer	
	<input checked="" type="checkbox"/> No		Released as from: /	<input type="checkbox"/> Internal
		<input type="checkbox"/> Flemish government		
		<input checked="" type="checkbox"/> Available online		

### Approval

Author	Reviser	Project Leader	Coordinator Research Group	Head of Division
Suzuki, T. 	Vantorre, M. 	Suzuki, T. 	Verwaest, T. 	Mostaert, F. 
Hassan, W. 				

### Revisions

Nr.	Date	Definition	Author(s)
1.0	3/02/2015	Concept version	Suzuki, T.; Hassan, W.
2.0	22/2/2015	Substantive revision	Vantorre, M.; Van Zwijnsvoorde, T.
3.0	14/04/2016	Revision customer	Meersschaut, Y.
4.0	10/06/2016	Final version	Suzuki, T.; Hassan, W.
5.0	21/10/2016	Adaptation confidentiality	Suzuki, T.

The Masterplan 'Vlaamse Baaien' outlines the need to develop an integrated vision for the Belgian coast. One of the Masterplan's goals is to achieve a win-win situation between coastal protection and the maintenance and improvement of the maritime access to the port of Zeebrugge.

The hinterland connection of the port of Zeebrugge by means of inland vessels is a major issue. Therefore, a specific type of inland vessels is conditionally allowed to make use of the 16 nautical miles long sea trajectory between Zeebrugge and the mouth of the Western Scheldt estuary to connect the port with the inland waterway network.

Detailed information about the wave climate in the area between the eastern dam of the port of Zeebrugge, Pas van het Zand, Scheur-Oost/Wielingen, Vlissingen, Breskens and the coastline is essential to maximize the efficiency of the sea-river traffic in the present situation, and to decrease the requirements of inland vessels for safe navigation on a coastal route between the port of Zeebrugge and the mouth of the Western Scheldt.

The existing project focuses on the model set-up and calculation of the detailed wave climate between Zeebrugge and the mouth of the Western Scheldt estuary in the present situation and also a future configuration for wind, wave and water level conditions throughout the year 2013 by means of the validated numerical model. The result of the simulation are delivered to the client for the further analysis (e.g. shading effects of new islands scenarios for the ship navigation).

Research results can be used for the further analysis of the navigation of all vessels which are making use of the present route and future alternative routes. Besides, it can serve as a basis to evaluate the impact of measures on the response of inland vessels.

---

## CONTENTS

Contents .....	I
List of tables.....	III
list of figures .....	IV
1 Introduction.....	1
1.1 Background.....	1
1.2 Aim of this study.....	2
1.3 Methodology .....	2
2 Numerical wave model.....	3
2.1 SWAN model.....	3
2.2 Model limitation .....	3
2.2.1 Introduction.....	3
2.2.2 Literature review .....	3
2.2.3 Summary.....	6
3 Available data .....	7
3.1 Data source.....	7
3.2 Data format (coordinate) .....	7
3.3 Data .....	7
3.3.1 Waves .....	7
3.3.2 Wind .....	8
3.3.3 Water level .....	9
3.3.4 Locations summary.....	9
4 The Belgian coast model.....	10
4.1 Introduction.....	10
4.2 Bathymetry / topography.....	10
4.3 Model performance.....	11
5 Model settings .....	12
5.1 SWAN version .....	12
5.2 Model domain and bathymetry.....	12
5.2.1 T0 calculation.....	12
5.2.2 A1 calculation .....	13
5.2.3 E1 calculation.....	13
5.3 Computational bin.....	14
5.4 Boundary conditions.....	14

5.4.1	Water level .....	14
5.4.2	Wave boundary condition .....	14
5.4.3	Wind conditions.....	15
5.5	Physical parameters .....	15
5.6	Numerical parameters.....	15
5.7	Output locations.....	16
5.8	Input example.....	16
6	Model results (T0).....	17
6.1	Validity of T0 model.....	17
6.2	Further optimization/calibration.....	18
6.3	Output of the model (T0) .....	19
7	Sensitivity analysis .....	21
7.1	Introduction.....	21
7.2	Model settings .....	21
7.2.1	Bathymetry and domain.....	21
7.2.2	Grid size and physical processes.....	21
7.2.3	Boundary conditions offshore .....	21
7.3	Model results.....	22
7.4	Computational cost .....	25
7.5	Conclusions.....	25
8	Simulation RESULTS FOR configuration E1.....	26
8.1	Bathymetry of E1.....	26
8.2	Validity of E1 model.....	26
8.3	Output of the model calculations for E1 .....	27
8.4	Example of spatial output for shading effect (E1).....	27
9	Conclusions.....	29
10	References .....	30
11	Appendix A.....	A1
12	Appendix B.....	A3

## LIST OF TABLES

Table 3-1: Directional waverider locations.....	7
Table 3-2: Wave parameters and description from directional waverider .....	8
Table 3-3: Measuring pile 0 at Wandelaar (MP0) .....	8
Table 3-4: Parameters and description from the measuring pile .....	8
Table 3-5: Tide measurement at Zeebrugge Leopold II dam (ZLD) .....	9
Table 4-1: Origin of the Belgian coast model .....	11
Table 5-1: Origin of the A1 and E1 configurations .....	13
Table 7-1: Overview of the wave height and period distribution at 5 m TAW at Knokke. ....	22



## LIST OF FIGURES

Figure 1-1: Part of the Flemish and Dutch coastline including the port of Zeebrugge and the mouth of Western Scheldt estuary (source: GoogleEarth).....	1
Figure 3-1: Locations of in situ measurement points.....	9
Figure 4-1: The domain and bathymetry contour plot in the Belgian coast model.....	10
Figure 4-2: Validity of the Belgian coast model in SWAN at Bol van Heist. (IMDC, 2009a).....	11
Figure 5-1: Bathymetry contour plot of T0 calculation and nesting boundary locations for A1 and E1 calculation. ....	12
Figure 5-2: Bathymetry contour plot for A1 calculation. The legend indicates the bathymetry level based on [m TAW].....	13
Figure 5-3: Bathymetry contour plot for E1 calculation. The legend indicate the bathymetry level based on [m TAW].....	14
Figure 5-4: Wave data output points for further analysis of ship navigation.....	16
Figure 6-1: Comparison between calculated and measured wave height at Bol van Heist, result of Deltares (personal communication with Marc Vantorre).....	17
Figure 6-2: Comparison between calculated and measured wave height at Bol van Heist, results of the present SWAN calculations.....	18
Figure 6-3: Location of Bol van Heist and E1 domain.....	19
Figure 6-4: Comparison between measured and calculated *(R, correction parameter) wave height at Bol van Heist, T0.....	20
Figure 6-5: Comparison between measured and calculated wave heights at Bol van Heist, scenario E1.....	20
Figure 7-1: Computed Hs [m] with various grid sizes (left: wave processes on, right: off) for configuration A1.	23
Figure 7-2: Hs difference between wave processes on and off. ....	23
Figure 7-3: Hs difference between 10 m grid and each grid. ....	24
Figure 7-4: Closer view on the tip of the island.....	24
Figure 8-1: Bathymetry contour plot as used in SWAN model computation of scenario E1. ....	26
Figure 8-2: Comparison of Hs between T0 (top panel) and E1 (bottom panel). ....	26
Figure 8-3: Wave shading effect by the new islands (wave dir.: NNW, NW, WNW, W).....	28
Figure 8-4: Wave shading effect by the new islands (wave dir.: NNW) combined with strong E wind.....	28

# 1 INTRODUCTION

## 1.1 Background

The Masterplan ‘Vlaamse Baaien’, submitted to the Flemish Government in May 2014, outlines the need to develop an integrated vision for the Belgian coast in a long term period, i.e. up to year 2100 (AMT, 2014). The main objective of this Masterplan is to investigate possible coastal interventions, that could ensure that the Belgian coast will be able to withstand the impact of climate change in terms of storms and floods, and remaining attractive in economic terms providing also opportunities for renewable energy production.

One of the Masterplan’s goals is to achieve a win-win situation between coastal protection at one side and the maintenance and improvement of the maritime access to the port of Zeebrugge at the other side (Figure 1-1). This coastal port is of significant importance. The hinterland connection of the port of Zeebrugge by means of inland vessels, however, is a major issue, especially for container traffic, due to the present restrictions of the inland canals between Bruges and Ghent. Alternatively, so-called *river-sea* ships, i.e. a specific type of inland vessels, are conditionally allowed to make use of the 16 nautical miles long sea trajectory between Zeebrugge and the mouth of the Western Scheldt estuary to connect the port with the inland waterway network (Vantorre et al., 2013).

However, the above mentioned *river-sea* vessels require a specific design with respect to construction and safety margins due to the wave induced loads and motions on the sea trajectory, which results in a higher investment for this type of vessel compared to ‘normal’ inland ships,. All measures which lead to a milder wave climate on the trajectory followed by the inland vessels – by creating a new route and/or protecting the inland navigation route from wave action – will therefore have a positive effect on the conditions which have to be imposed to inland ships to allow safe traffic on a coastal route. One possible idea is to create another new entrance for inland navigation through the eastern dam to avoid high wave conditions in front of the entrance of the port of Zeebrugge.

In order to maximize the efficiency of the *sea-river* traffic in the present situation detailed information about the wave climate in the area between the eastern dam of the port of Zeebrugge, Pas van het Zand, Scheur-Oost/Wielingen, Vlissingen, Breskens and the coastline is essential. In addition, this information can lead to a decrease of the requirements of inland vessels for safe navigation on the coastal route between Zeebrugge and the mouth of the Western Scheldt.



Figure 1-1: Part of the Flemish and Dutch coastline including the port of Zeebrugge and the mouth of Western Scheldt estuary (source: GoogleEarth).

## 1.2 Aim of this study

The present study will focus first on the model set-up. Next calculations of the detailed wave climate between Zeebrugge and the mouth of the Western Scheldt estuary in the present situation and also for a future configuration are carried out. Therefore, a validated numerical model for all wind, wave and water level conditions throughout the year 2013 (i.e. the Belgian coast model in SWAN developed in the project R769\_01) will be applied. This output can be used for the further analysis for the navigation of the vessels making use of the present route and future alternative routes, and can serve as a basis to evaluate the impact of measures on the response of inland vessels. Therefore in this report, no further analysis is conducted after the computation of T0 and E1 configuration. All results are delivered to the client for further analyses.

## 1.3 Methodology

The *wave transformation matrix* developed by KULeuven/WLH (2004) and IMDC (2006) has not been used in this study since the output locations are limited in those calculations, and the shape of the offshore spectrum is assumed a priori and the interpolation might introduces an additional uncertainty as stated in IMDC (2006). Furthermore this model cannot be applied to the future configuration.

Instead of using the wave transformation matrix, we use the Belgian coast model in SWAN. This model gives reliable result in terms of wave propagation for the present configuration. Even though it gives a good result already, we conducted a further modification/calibration of the output results based on the measured waves at Bol van Heist. The calculated and calibrated results are used for calculation of wave transformation in a future configuration.

The flow of the present study and associated chapter are shown below.

1. Literature review (Chapter 2)
2. Data collection (Chapter 3)
3. Model setting (Chapter 4,5)
4. Validation of the model (Chapter 6)
5. Wave climate in T0, present configuration (Chapter 6)
6. Sensitivity analysis for island configuration (Chapter 7)
7. Wave climate in E1, future configuration (Chapter 8)

## 2 NUMERICAL WAVE MODEL

### 2.1 SWAN model

SWAN (Simulating WAVes Nearshore) is a third-generation wave model, developed at Delft University of Technology, which computes random short-crested wind-generated waves in coastal regions and inland waters (Booij et al., 1999). This model is based on the numerical solution of the wave action balance equation and accounts for physics such as wave propagation, shoaling refraction, wave generation by wind, transmission through and reflection against obstacles, and diffraction.

### 2.2 Model limitation

#### 2.2.1 Introduction

It has to be noted that wave diffraction is modelled in a simplified manner, by use of a phase-decoupled refraction-diffraction approach proposed in Holthuijsen et al. (2003), in order to describe (qualitatively rather than quantitatively) the behavior of spatial variation in wave direction.

Wave diffraction is the process by which energy spreads laterally perpendicular to the dominant direction of wave propagation and mainly occurs when waves come up against natural or artificial obstacles (shoals, islands, peninsulas, breakwaters etc.). Therefore, diffraction is responsible for the transmission of wave disturbance to the sheltered side (or shadow zone) of the obstacle.

In this section the performance of SWAN model is investigated in simulating wave diffraction adequately, through a review of relevant research studies that have been done recently. The reason is that SWAN is intended to be utilized for the simulation of the wave climate in the coastal zone east of Zeebrugge port, within this study, which will investigate a new scenario of intervention around the existing eastern breakwater. It is expected that these measures will provide safer and easier access of inland navigation vessels to the port. Although the majority of the published studies refer to cases of breakwater-like structures, useful information about the performance of SWAN in wave diffraction process can be extracted.

#### 2.2.2 Literature review

##### [Holthuijsen et al. \(2003\)](#)

In this paper, the approach to add a wave diffraction term obtained from the mild-slope equation, in the action balance equation, numerically solved by SWAN, is presented. The main drawback of this approximation is that phase information is omitted and therefore, coherent wave fields developed in harbors (standing-wave patterns) cannot be simulated. Three cases of bottom and structure geometries, i.e. an elliptical shoal, a semi-infinite breakwater and an infinite breakwater with a gap (both fully reflective), were simulated in order for the proposed method to be verified. For the case of the elliptical shoal two cases were considered: one with monochromatic, unidirectional waves and one with random, long-crested waves. Numerical predictions from both wave cases showed that the phase-decoupled approximation hardly affects the maximum wave height but it increases the minimum wave height at the sheltered area behind the shoal (spreading the effect of the shoal over a slightly larger area), compared to SWAN results without diffraction. For the case of the semi-infinite breakwater, perpendicular, monochromatic but also short-crested waves were considered. Results presented only for the case of the unidirectional waves, were compared to the analytical Sommerfeld solution and it was found that the phase-decoupled approach reproduces reasonably well near the shadow line and in the exposed region, much better than without diffraction, but still the wave energy deep in the shadow area is underestimated. It is mentioned that similar conclusions can be made for the case of short-crested waves (with directional spreading widths of  $10^\circ$  and more),

where diffraction effects are expected to be considerably reduced (though results are not presented). Finally, for the case of the gap in infinite breakwater, the comparison among numerical results of SWAN with and without diffraction, the Sommerfeld solution and laboratory measurements showed that the phased-decoupled approach performed reasonably well also only when singularities at the tips of the breakwaters were accommodated in the approach.

Concluding, it is mentioned that the numerical results, overall, agree reasonably well with measurements and analytical models, even in these extreme diffraction-prone conditions. The application of the proposed approximation is only limited by the absence of phase-coupling in the wave fields (no coherent wave fields are simulated). In real conditions, such coherent wave fields may occur when the wave reflection off obstacles is done in a coherent manner. This implies that the proposed phase-decoupled approximation should not be used if:

- (a) an obstacle or a coastline covers a significant part of the down-wave view, and in addition,
- (b) the distance to the obstacle or coastline is small (less than few wavelengths), and in addition,
- (c) the reflection of that obstacle or coastline is coherent, and in addition,
- (d) the reflection coefficient is significant

Overall, the proposed diffraction approximation can be used in most situations near absorbing or reflecting coastlines with an occasional obstacle such as islands, breakwaters, or headlands but not in harbors with standing waves or near wall-defined cliff walls. The coastline may be fully reflecting as long as the reflection is incoherent (e.g. irregular blocks, rocks or reefs that are small compared to the wave length) as incoherent reflection can be accounted for separately by SWAN.

#### The SWAN team (2015)

The Scientific and Technical Documentation for SWAN Cycle III version 41.01A refers to the aforementioned phase-decoupled refraction-diffraction approach, which is mostly based on the work presented in Holthuijsen et al. (2003), so only the additional information is reported in the present memo.

It is referred that in irregular, short-crested wave fields it seems that the effect of diffraction is small, except in a region less than one or two wavelengths away from the tip of the obstacle (Booij et al., 1993). Therefore the model can reasonably account for waves around an obstacle if the directional spectrum of incoming waves is not too narrow, unless one is interested in the wave field deep into the shadow zone. Furthermore, it is mentioned that the phase-decoupled approximation in SWAN model is not valid in front of reflecting breakwaters, but it can be used behind breakwaters (even reflecting ones), as long as the conditions mentioned in the last paragraph of the previous section are met.

#### Enet et al. (2006)

The simple case of a semi-infinite breakwater, with zero reflection and zero transmission, in water of constant depth, omitting the growth by wind and bottom dissipation, is investigated for evaluating the performance of diffraction in SWAN (version 40.51). Three cases of short-crested waves with rms energy weighted spreading of  $\sigma = 1.5^\circ$  (unidirectional),  $\sigma = 10^\circ$  (swell) and  $\sigma = 30^\circ$  (wind waves), are considered. The tests that are performed include (among others) the estimation of the spatial resolution and the computational domain size effect. Then, the comparison against an analytical solution, the determination of the areas where diffraction is important and the evaluation of the role of directional spreading on the results, take place. No safe conclusions about spatial resolution can be made, due to unstable results for grids with more than 3.5 cells per wavelength. One of the main conclusions of this study is that for situations with narrow directional spectra (say less than  $15^\circ$ ),

the SWAN model should be used with diffraction, whereas in situations with wide spectra, it seems to be better to use SWAN without diffraction. However for the case of  $\sigma = 30^\circ$ , in the area immediately behind the breakwater the result with diffraction is significantly better than the result without diffraction.

### Boshek (2009)

One of the objectives of this study (M.Sc. thesis) is to test the ability of SWAN (version 40.72) to simulate diffraction around breakwaters, i.e. a semi-infinite one and a breakwater gap, over a flat, deep bottom. Wave forcing conditions are determined by JONSWAP spectra of  $\gamma = 3.3$  for wind waves and  $\gamma = 10$  for swell, and a directional spreading of  $\sigma = 30^\circ$  and  $\sigma = 10^\circ$  for wind waves and swell, respectively. The peak wave period,  $T_p$ , is considered equal to 8 s. Firstly, a sensitivity analysis for the main model properties is performed, showing that the directional resolution of  $\Delta\theta = 2^\circ$  resulted into smoother results than the one of  $\Delta\theta = 10^\circ$ , so the first one is chosen for all the simulations. As for the grid resolution, 4 grid cells per wavelength are chosen, since diffraction computations in SWAN presented instabilities in the vicinity of the breakwater tip for 5 grid cells per wavelength. Furthermore, tests with diffraction and without diffraction showed that only the first case most closely represents diffraction characteristics. It appears from this analysis that by removing diffraction from the computation, the wave energy does not change direction against the leeside of the breakwater as expected. The combined effects of diffraction and reflection are not investigated in detail, consequently only the diffraction approximation of the model without reflection is compared to analytical results. It is found that for both cases of breakwaters, the similarity between SWAN and Goda's irregular diffraction diagrams is stronger for broadly directed waves than for narrow directional waves. Overall, this comparison revealed good congruency with only significant differences in the area directly behind the breakwater.

### Lin (2013)

In this study an improved version of the phase-decoupled refraction-diffraction approach coupled with SWAN model is presented, so that cases of steep varying sea bottoms can also be simulated. This is achieved by adjusting the diffraction correction parameter introduced by Holthuijsen et al. (2003), including the effect of higher-order bottom slope terms and the wave-bottom and wave-current interaction.

Verification of the new model is not included due to the lack of corresponding field observations, hydraulic model tests and numerical simulations, therefore only comparisons of the numerical results from SWAN ver. 40.72 and the new modified version are presented. Three different bathymetries, i.e. a flat bottom and two bottoms of slope 1:100 and 1:50, and three layouts, i.e. a semi-breakwater, breakwaters with gap, and a detached breakwater were used in the afore-mentioned comparisons. Wave forcing conditions are determined by a JONSWAP spectrum ( $\gamma = 3.3$ ) and a directional spreading parameter  $m = 2$  ( $\sigma = 31.5^\circ$ ) for short-crested random waves and  $m = 50$  ( $\sigma = 8.0^\circ$ ) for long-crested random waves (cos-m distribution), while the cases with wave period  $T_S = 6$  s, 8 s, and 10 s are considered. After comparison between the original and the modified version of SWAN it was found that, for the case of the semi-infinite breakwater (of all bathymetries), only for long-crested random wave cases, the numerical results have varied as the incident wave periods become longer. In the case of the breakwaters with a gap, where the diffraction effect is stronger than the other two layouts, the two models have great differences in all wave cases, especially when the wavelength (or wave period) is longer than the opening width. In the detached breakwater cases, the two versions have almost the same results in short-crested wave cases, however, in long-crested wave cases, the difference between the two versions increases when the relative water depth becomes shallower and there are long period waves. In general, the modified version overcomes numerical instability problems (in specific cases) faced in the original version.

### Rusu et al. (2008)

This study refers to the evaluation of the wave conditions in Madeira Archipelago (Portugal) by use of spectral models, i.e. WAM (for wave generation) and SWAN (for coastal wave transformation). Specifically, in order to simulate wave generation and propagation from deep ocean to coastal environment, the idea to nest into the ocean-scale models higher resolution models able to account better for the nearshore physics is adopted. However, the study focuses on the effects of diffraction and triad nonlinear interactions resulting from the simulations performed by SWAN (version 40.51), emphasizing the influences induced in the model results when increasing the spatial resolution. For this reason two levels of computational grids were constructed, a medium- (2nd level) and a high-resolution (3rd level) grid. The first case study reflects the effect of a high-energetic situation in the coastal wave climate of Madeira and Porto Santo islands, where the process of diffraction is analyzed, by comparing results of SWAN runs with diffraction and without diffraction. It is found that the results are sensitive to the spatial resolution and while for the 2nd level a maximum relative increase in the significant wave height of about 36% is encountered, for the 3rd level a relative increase of about 60% in the significant wave height occurs. For the case of Porto Santo island the corresponding relative increase between the two levels of grids are smaller than the case of Madeira (two peaks of 30% and 38% at the 2nd level and 44% at the third level). In average energetic conditions variations of 0.2–0.3m in the significant wave height (in general positive biases) were encountered in the model results when the diffraction command was activated, sometimes meaning a relative increase in the significant wave height field greater than 30%.

#### 2.2.3 Summary

The evaluation of SWAN as a model capable in accounting for the process of wave diffraction, was investigated through a review to relevant research studies that has been done recently. Wave diffraction is modelled in a simplified manner in SWAN, by use of a phase-decoupled refraction-diffraction approach proposed in Holthuijsen et al. (2003) and it is obtained from the mild-slope equation. The majority of the published studies presented here, refer to cases of breakwater-like structures, and only one case of diffraction referred to islands. The main conclusion of Holthuijsen et al. (2003) is that the proposed diffraction approximation can be used in most situations near absorbing or reflecting coastlines with an occasional obstacle such as islands, breakwaters, or headlands but not in harbors with standing waves or near wall-defined cliff walls. For the case of a semi-infinite breakwater, Enet et al. (2006) concluded that for situations with narrow directional spectra, the SWAN model performed better with the diffraction mode on, whereas in situations with wide spectra, SWAN performed better only in the area immediately behind the breakwater. Boshek (2009) found that the similarity between SWAN and Goda's irregular diffraction diagrams is stronger for broadly directed waves than for narrow directional waves, for both cases of a semi-infinite breakwater and a gapped breakwater. Lin (2013) proposed a modified version of the phase-decoupled refraction-diffraction approach, in order to account for varying sea bottoms. In general, this modified version seems to overcome numerical instability problems faced in the original version for the afore-mentioned types of breakwaters. Finally, Rusu et al. (2008) concluded that the grid resolution influences substantially the diffraction after conducting simulations by use of SWAN in the coastal area of Madeira and Porto Santo islands in Madeira archipelago.

Still there is some uncertainties for the behavior of diffraction, a sensitivity analysis of grid resolutions is conducted for this study to know which grid resolution is suitable for the calculation of future configuration, since it includes islands where diffraction effect plays an important role for wave transformation.

## 3 AVAILABLE DATA

### 3.1 Data source

In situ wave data and wind data are obtained from *Meetnet Vlaamse Banken* operated by Hydrography department of the Coastal division. Normally, only wave parameters can be obtained in terms of wave data but in this study full wave spectrum data was specially requested to Coastal division and obtained through personal communication (Hans Poppe, 8 October 2015). For this study the data of 2013 (entire year) is collected and used.

Bathymetry data for present T0 configuration is extracted from the Belgian coast model (dx = dy = 250 m grid). Bathymetry data for future A1 and E1 configurations are generated by combining present T0 bathymetry with new island bathymetries received from the Maritime Access division.

### 3.2 Data format (coordinate)

The data format (coordinate) used in this study is [m in WGS84UTM31] in horizontal axis (x- and y-direction) and [m TAW] in vertical axis (z-direction). All the obtained data have been transformed into this data format to proceed further calculations and analyses.

### 3.3 Data

#### 3.3.1 Waves

Measured wave data (statistical wave parameter obtained every 30 minutes) obtained by directional waveriders at three locations, at Westhinder, ZW-Akkaert and Bol Van Heist are used in the present study. The coordinate of the locations of the directional waverider are summarized in Table 3-4. Note that the coordinate information is extracted from the website of the Meetnet Vlaamse Banken at the moment of 2015.

The wave parameters obtained at those locations are summarized in Table 3-2. The wave measurement from the Meetnet Vlaamse Banken is first processed as wave spectrum data (full spectrum; directional components + frequency components) from the measurement, and eventually translated into wave parameters. Normally parameters are only used for further analysis/simulations but in this study measured full wave spectrum is used for the input in the SWAN model since it is supposed to be more accurate (including more information).

Table 3-1: Directional waverider locations

Location	Location code	Coordinate (N)	Coordinate (E)
Westhinder	WHI	51° 22' 51"N	2° 26' 20"E
ZW-Akkaert	AKZ	51° 24' 58"N	2° 49' 07"E
Bol Van Heist	BVH	51° 23' 30"N	3° 12' 01"E



Table 3-2: Wave parameters and description from directional waverider

Parameter Code	Omschrijving	Eenheid
E10	Laagfrequente golfenergie (0.03 Hz - 0.1 Hz)	cm <sup>2</sup> .s
GEM	Energie maximum van het spectrum	cm <sup>2</sup> .s
GTZ	Gemiddelde golfperiode	s
HLF	Hoogte golven met een periode > 10 seconden	cm
HMO	Significante golfhoogte berekend uit het spectrum	cm
HM1	Gemiddelde hoogte 10% hoogste golven berekend uit het spectrum	cm
HMM	Gemiddelde golfhoogte berekend uit het spectrum	cm
REM	Richting van de frequentiecomponent met de hoogste energie	graden
RHF	Richting van de hoogfrequente golven (periode tussen 2 en 5 seconden)	graden
RLF	Richting van de laagfrequente golven (periode groter dan 10 seconden)	graden
TPE	Periode van de golven met de hoogste energie	s
TZW	Zeewatertemperatuur	°C
SEM	Spreadingshoek van de frequentiecomponent met de hoogste energie	graden

### 3.3.2 Wind

Wind measurement data (every 10 minutes) at the measuring pile 0, Wandelaar (MP0) in 2013 are again obtained from the Meetnet Vlaamse Banken. The coordinate of the location is shown in Table 3-3. The parameters and description are shown in Table 3-4. Average wind speed and direction are used applying a correction factor for this study, because the input for the SWAN model is the average wind speed at the height of 10 m from the sea level.

Table 3-3: Measuring pile 0 at Wandelaar (MP0)

Location	Location code	Coordinate (N)	Coordinate (E)	Measurement height
Wandelaar	MP0	51° 23' 40"N	3° 02' 44"E	25.73 m

Table 3-4: Parameters and description from the measuring pile

Data	Parametercode 10-minuut data (herh.tijd=010)	Eenheid data	Opmerkingen
- Gemiddelde windsnelheid	WVS	m/s	
- Max. 3sec windstoot	WG3	m/s	
- Max. 1sec windstoot	WG1	m/s	Enkel op de meteoparken
- Gemiddelde windrichting	WRS	°	

### 3.3.3 Water level

Water level data (every 5 minutes) used in this study are obtained by tide measurement station at Zeebrugge Leopold II dam (ZLD). The coordinate of the location is shown in Table 3-5.

Table 3-5: Tide measurement at Zeebrugge Leopold II dam (ZLD)

Location	Location code	Coordinate (N)	Coordinate (E)
Zeebrugge Leopold II dam	ZLD	51° 20' 46"N	3° 12' 01"E

### 3.3.4 Locations summary

All locations used in this study (WHI; AKZ; MP0; BVH; ZLD) are shown in Figure 3-1.

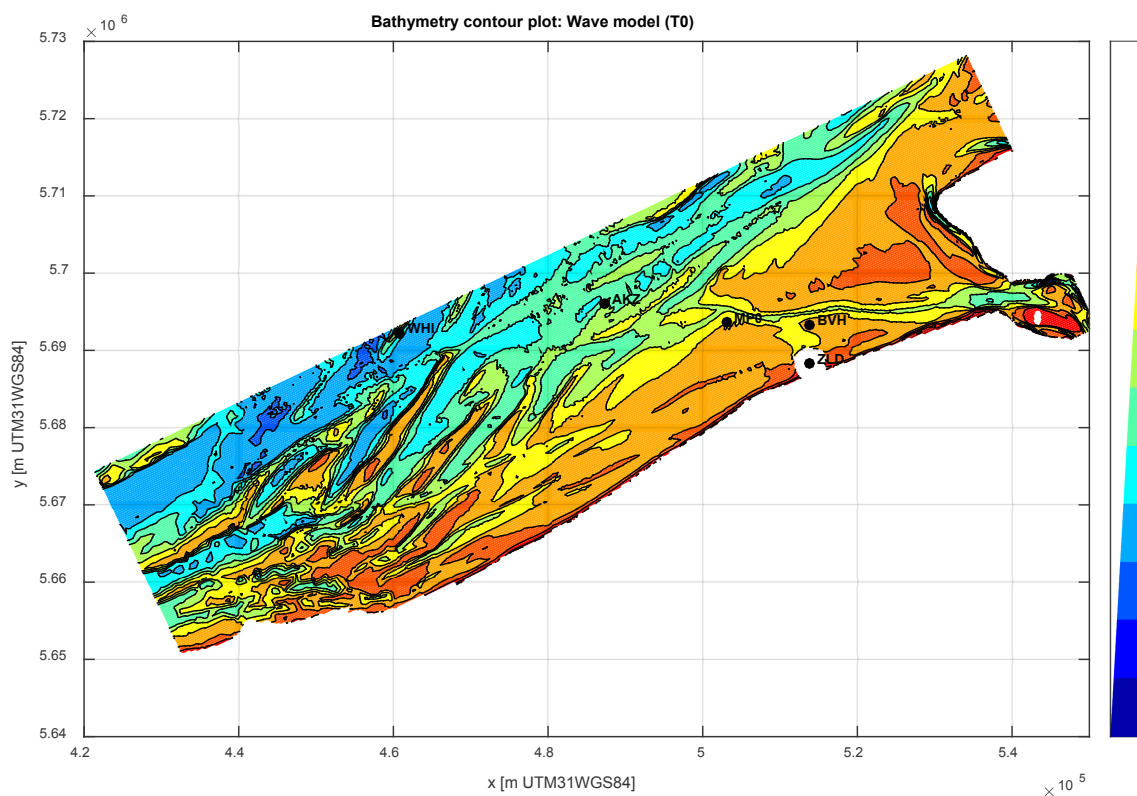


Figure 3-1: Locations of in situ measurement points

## 4 THE BELGIAN COAST MODEL

### 4.1 Introduction

The *Belgian coast model* has been studied intensively (e.g. Verwaest et al. 2008; IMDC 2005; 2006; 2008; 2009a; 2009b; 2009c) and validated poorly (because no REF?). The model has also been applied to coastal projects in Belgium (e.g. Coastal safety master plan). It should be noted that the validated SWAN model based on the project R769\_01 in FHR is named as 'Belgian coast model'.

### 4.2 Bathymetry / topography

The bathymetry of the Belgian coast model is shown in Figure 4-1. The grid size for x-direction and y-direction is equivalent and is both 250 m for one grid cell and the number of grids are 156 and 500, respectively. This bathymetry is used for the simulation of T0 configuration (T0 = present configuration in 2002, see details in De Roo et al., 2015). Note that we have omitted the differences between the bathymetry of 2002 and 2014 (current bathymetry since the differences are small enough looking at the very rough grid resolution, 250 m x 250 m grid, used in this study. The small differences are averaged out. Table 4-1 shows the origin and grid information in the Belgian coast model.

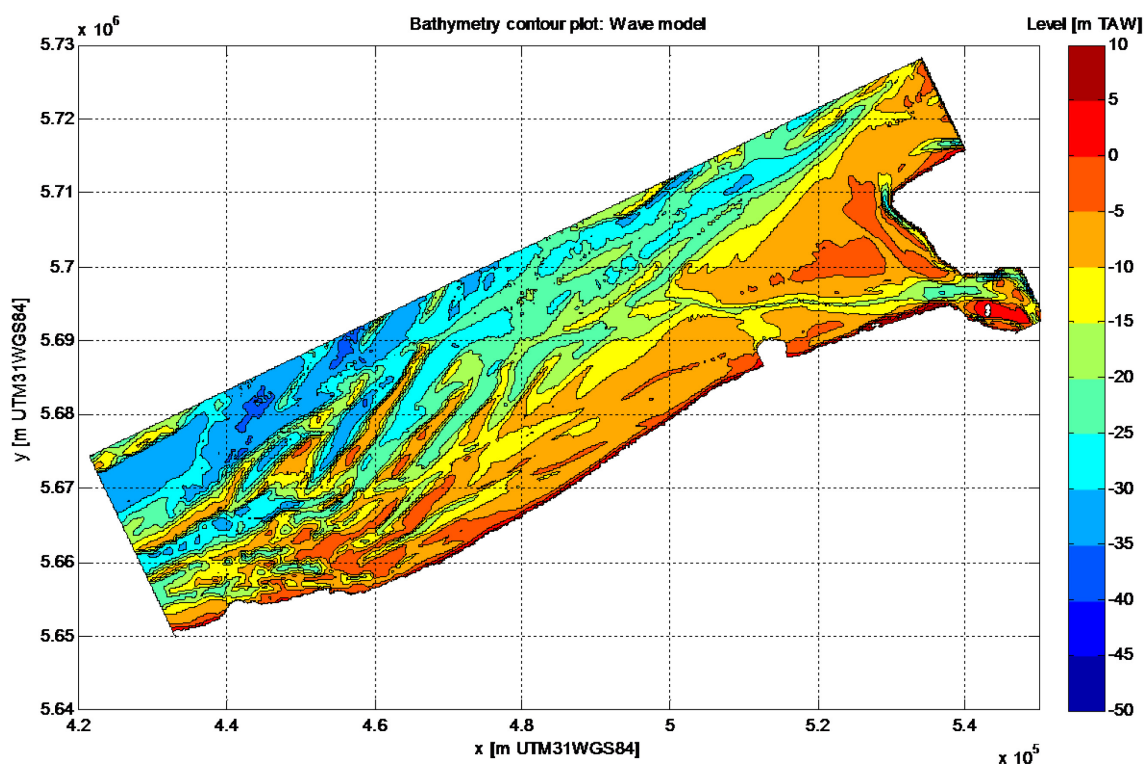


Figure 4-1: The domain and bathymetry contour plot in the Belgian coast model

Table 4-1: Origin of the Belgian coast model

Description	X coordinate (WGS84UTM31)	Y coordinate (WGS84UTM31)	Rotation	Number of grid in x	Number of grid in y
Origin of the Belgian coast model	438116.00	5639190.00	25.50	500 (dx=250 m)	156 (dy=250 m)

### 4.3 Model performance

Figure 4-2 presents the results of the model validation with measured field data at BVHD (BVH Directional waverider; this abbreviation BVHD is the detailed expression including the information of measurement equipment *directional waverider*). Although there is clear scatter, the model reproduces the measured Hm0 values very well statistically: the linear trend line between measured values and model outcomes is almost equal to the 1:1-bissectrice.

The grid sizes in x- and y- direction are both 250 m and the number of grids are 156 and 500, respectively as stated earlier and the CPU time for one run (with a single core) in SWAN is about 30 min.

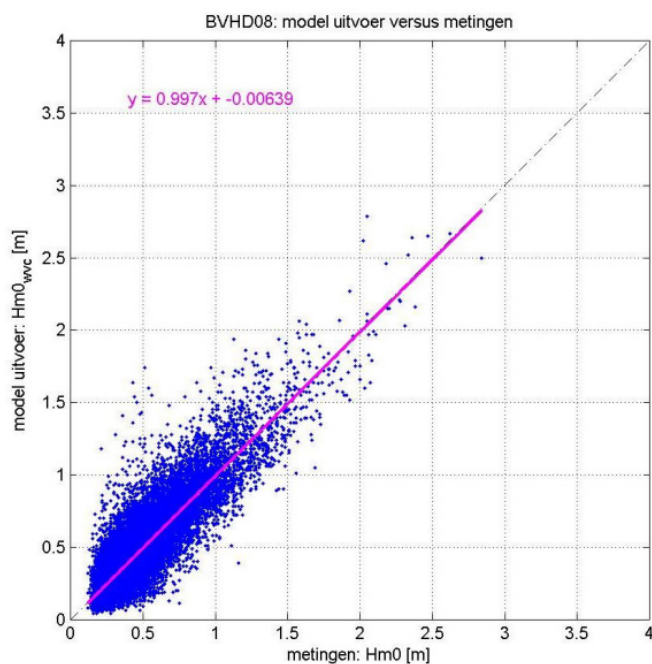


Figure 4-2: Validity of the Belgian coast model in SWAN at Bol van Heist. (IMDC, 2009a)

## 5 MODEL SETTINGS

### 5.1 SWAN version

SWAN version of 40.85 is used for all calculations in this study. Note that there is no significant change between version 40.85 and 40.72 which was used earlier in the Belgian coast model.

### 5.2 Model domain and bathymetry

#### 5.2.1 T0 calculation

Basic settings (e.g. model domain, bathymetry, grid size) of T0 calculation are the same as used in the Belgian coast model. The hydraulic and wind boundary conditions applied in this study are from the year 2013.

For the calculation of future bathymetry (i.e. A1 and E1 configurations) the ‘nesting’ method in SWAN is used, see details in SWAN team (2015). Since reflection has not been included at the land boundaries in the Belgian coast model, there are no reflected waves in the computational domain. SWAN only calculates incident waves, and that is a reason why the nesting calculation works. The nesting boundary locations used for A1 and E1 calculations are shown as a black box in Figure 5-1.

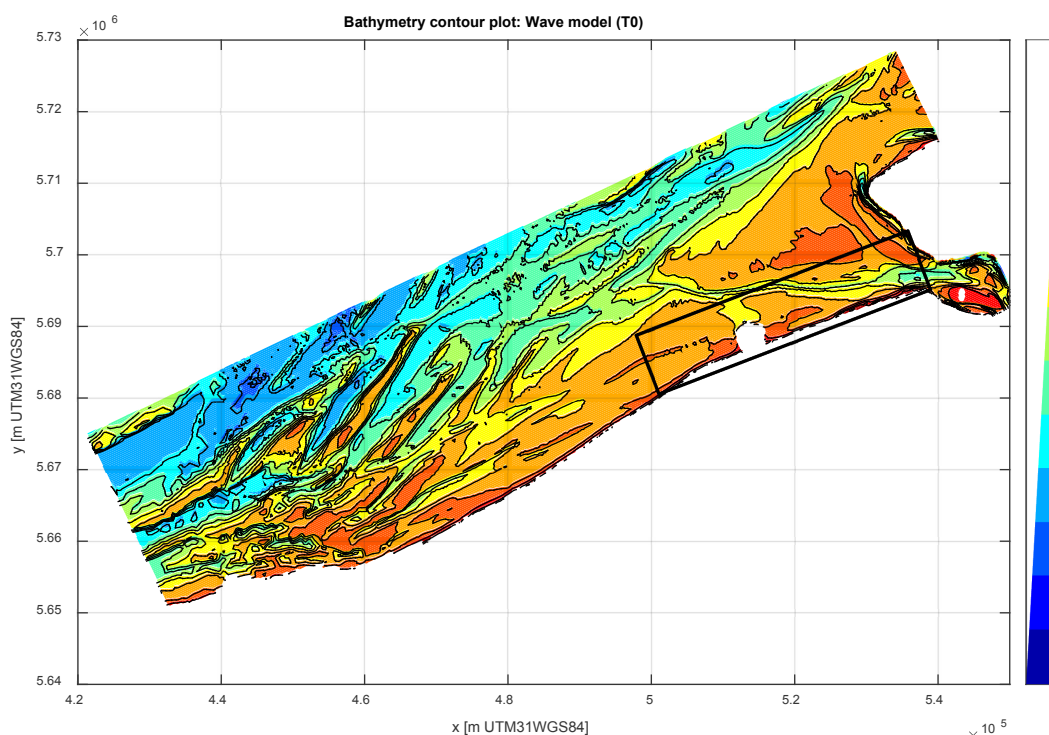


Figure 5-1: Bathymetry contour plot of T0 calculation and nesting boundary locations for A1 and E1 calculation.

### 5.2.2 A1 calculation

A1 configuration shown in Figure 5-2 has been used only for the sensitivity analysis. Note that the A1 bathymetry file is developed based on the data provided from Maritime Access Division (personal communication with D. Renders on 14/09/2015). As can be seen in the figure, the bathymetry around the Zeebrugge is from Maritime Access Division and the other part is based on the T0 bathymetry. Table 5-1 shows the origin (x and y position in WGS84UTM31 coordinate) and the bathymetry information (rotation and number of grids for x and y direction, and dx, dy) for A1 and E1 scenarios. For both case, the computational domain is exactly the same (same origin x and y, and the same length). Only differences are the level of the bathymetry and island configuration. Note that 10 m grid is not directly used in the computation since it requires a huge computational cost. Instead 50 m grid is used which has been chosen based on a model sensitivity analysis. Therefore the information shown in Figure 5-2 is only used as model input.

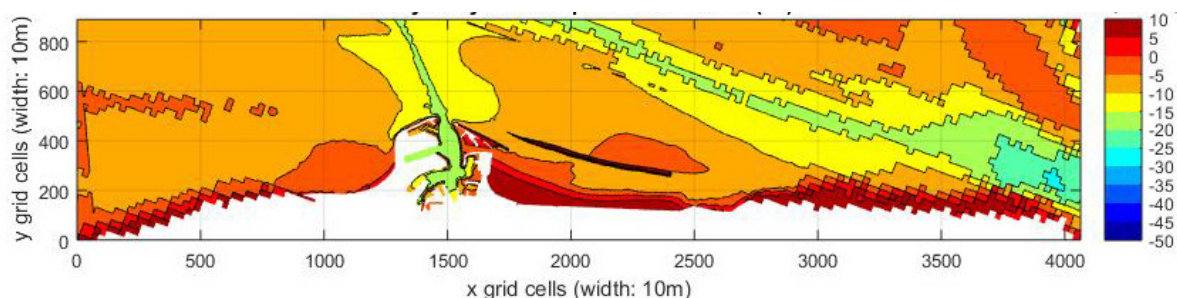


Figure 5-2: Bathymetry contour plot for A1 calculation. The legend indicates the bathymetry level based on [m TAW]

Table 5-1: Origin of the A1 and E1 configurations

Description	X coordinate (WGS84UTM31)	Y coordinate (WGS84UTM31)	Rotation	Number of grid in x*	Number of grid in y*
Origin of the A1 and E1 configurations	501058.00	5680545.00	21.04	4060 (dx=10 m)	880 (dy=10 m)

\*Those are only used for the input in SWAN.

### 5.2.3 E1 calculation

E1 configuration as shown in Figure 5-3 has been used for the final model run. Note that 10 m grid is not directly used in the computation since it requires a huge computational cost. Instead 50 m grid is used which has been chosen based on a model sensitivity analysis (as explained/described where?). Note that the E1 bathymetry file is again derived with the data provided from Maritime Access Division (personal communication with D. Renders on 17/12/2015). As can be seen in the figure, the bathymetry around the Zeebrugge is from Maritime Access Division and the other part is based on a smoothed T0 bathymetry.

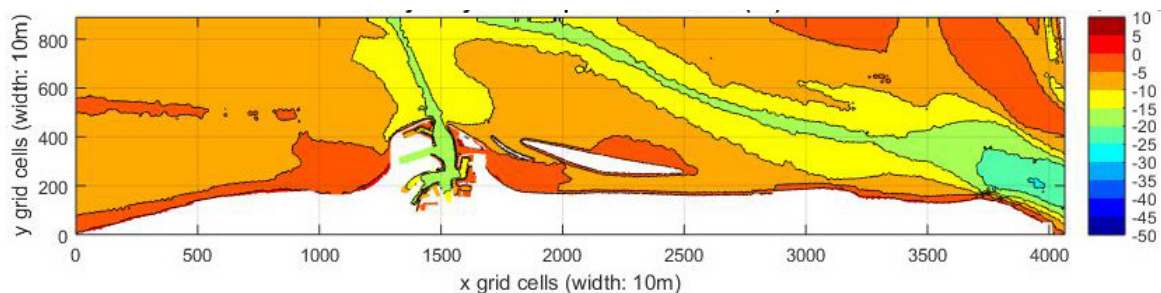


Figure 5-3: Bathymetry contour plot for E1 calculation. The legend indicate the bathymetry level based on [m TAW]

## 5.3 Computational bin

Frequency band in the SWAN calculation is selected between 0.025 and 0.85 Hz ( $T \sim 1.2$  s to 40 s) with 37 bin (=the frequency is divided into 37 discrete energy portion). Directional resolution is set as 10 degrees. This is common for all calculations in the present study.

## 5.4 Boundary conditions

### 5.4.1 Water level

The measured water levels at ZLD are used as a boundary condition for T0 and E1 calculations.

The in situ water level data were recorded every 5 minutes. In the present study, the measured water level every 2 hours has been used in SWAN model computations. The used data starts at +02:00 hours in 2013. This is a common setting for all scenarios calculations (i.e. T0 and E1 cases) in this study.

### 5.4.2 Wave boundary condition

#### T0 calculation

Measured wave spectra at AKZ are used as wave boundary conditions in the T0 calculation. The use of AKZ instead of WHI is one of the conclusions after the validation study of IMDC (2009a). The available wave spectrum data was collected every 30 minutes and is filtered in the present study to obtain wave parameters every 2 hours.

Averaged values of the previous 1 hour of each time step is used (2 data points before each time step) based on the study of IMDC (personal communication with Koen Trouw on 2 October 2015). In this way we can take into account the wave travelling time from deep water to the area of interest close to the shoreline at BVHD.

- Spec 1 e.g. 0:00
- Spec 2 e.g. 0:30
- Spec 3 e.g. 1:00
- Spec 4 e.g. 1:30
- Spec 5 e.g. 2:00 (Spec 3+ Spec 4) / 2 is used for calculation at 2:00

## A1 calculation

A1 model runs are used for the sensitivity analysis. The main purpose of the sensitivity analysis is to get acceptable grid resolution for E1 calculation. Simplified wave boundary conditions have been used in this sensitivity analysis.

## E1 configuration

Nesting data obtained in the T0 calculations has been applied.

### 5.4.3 Wind conditions

The in situ wind data was recorded every 10 minutes. It was also recommended to adjust the wind speed at the model boundary by taking the averaged value of 30 minutes previous to each time step (personal communication with Koen Trouw on 2 October 2015) in order to take into account the history effects of wind. This means using an average value of 3 points before the selected time step.

- Wind 1 e.g. 1:30
- Wind 2 e.g. 1:40
- Wind 3 e.g. 1:50
- Wind 4 e.g. 2:00      (Wind 1+ Wind 2 + Wind3) / 3 is used for calculation at 2:00

The wind data is obtained at the height of 25.7 m TAW. Therefore wind speed needs to be modified using log-law when it is applied to SWAN, in which the model input should be the wind speed at 10 m high from MSL. In this study the correction coefficient of  $R=0.94$  is used. It is also recommended from the previous study (personal communication with Koen Trouw on 2 October 2015) that the wind speed is also corrected according to the wave height ( $H_s$ ). The wind speed correction factor  $R = 0.94$  for large waves  $H_s > 1.0$  m and  $R = 0.8$  for small waves  $H_s < 1.0$  m.

Wind growth was computed using WESTHUYSEN instead of the method of Komen as in the original SWAN model setting.

Those above mentioned settings are used for all scenario calculations (i.e. T0 and E1 cases) in the present study.

## 5.5 Physical parameters

Wave breaking and bottom friction are activated with default values for all calculations in this study.

For the future configuration runs (A1 and E1 calculations), diffraction and triad (wave-wave interaction) are activated with a default value as well.

## 5.6 Numerical parameters

Computation is stopped after maximum 50 iteration steps.



## 5.7 Output locations

In total 150 locations have been selected to obtain the output results of SWAN model runs. These locations are presented in Figure 5-4 and the coordinates of these locations are given in Appendix A.

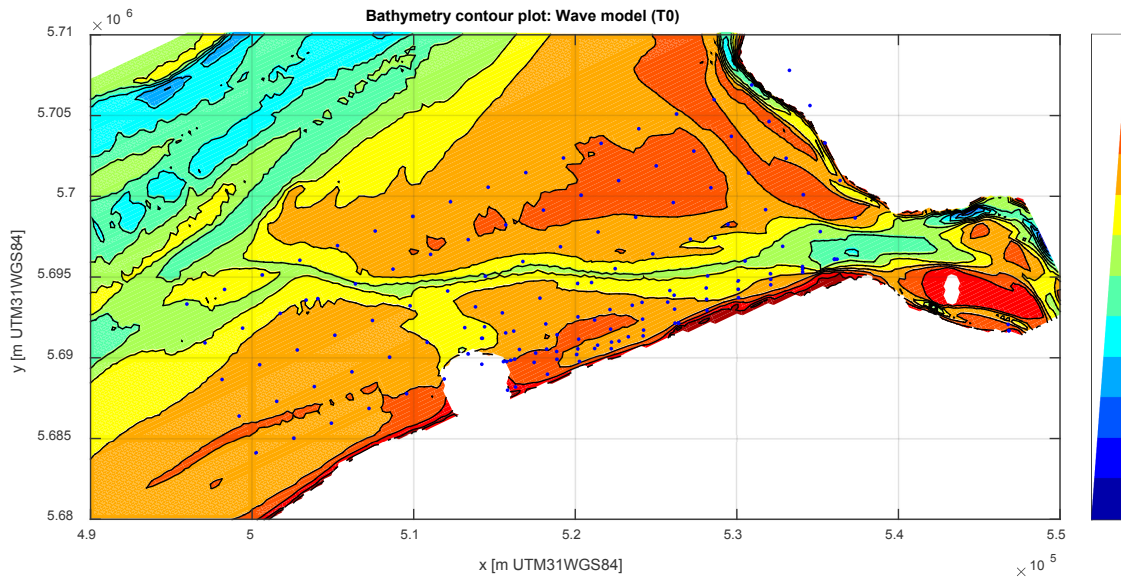


Figure 5-4: Wave data output points for further analysis of ship navigation

## 5.8 Input example

Input example is shown in Appendix B.

## 6 MODEL RESULTS (T0)

### 6.1 Validity of T0 model

The model quality can be checked by comparing calculated and measured significant wave heights (Hs) at Bol van Heist. If wave transformation and wind wave generation are modelled in a good way, wave height estimates at Bol van Heist would show a good agreement with the measurement data.

Figure 6-1 shows the model result from the runs calculated by Deltares (personal communication with Marc Vantorre, on 9 October 2015). This is one year significant wave height estimation for 2013. At first glance, the model shows a good performance.

Figure 6-2 shows the Belgian coast model used in this study. Again, one year significant wave height estimates are shown for 2013. A total of 4380 data points, namely data every 2 hours for 1 year, have been applied to estimate wave climate. However, due to the lack of data / incompleteness of the data, not all the data points have been calculated. As a result in total 3558 data points have been calculated. The model in the present study shows a good performance, even slightly better in terms of linear trend line (Deltares  $y=0.84x+0.17$ ; in this study  $y=0.91x+0.04$ ) and also  $R^2$  value (Deltares  $R^2=0.82$ ; in this study  $R^2=0.88$ ).

Therefore it can be concluded that T0 model developed in this study gives a good/better estimation of wave height at least till Bol van Heist. It is decided that it can be used for the calculation of possible alternative situations, namely E1 configuration.

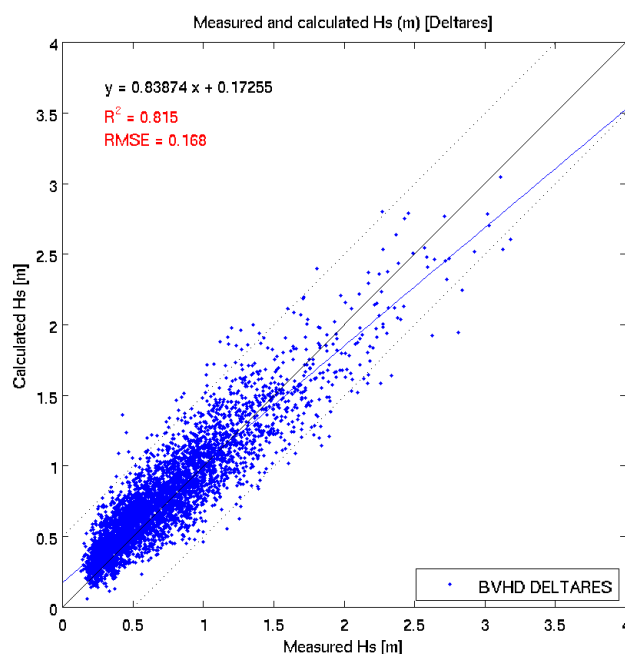


Figure 6-1: Comparison between calculated and measured wave height at Bol van Heist, result of Deltares (personal communication with Marc Vantorre).

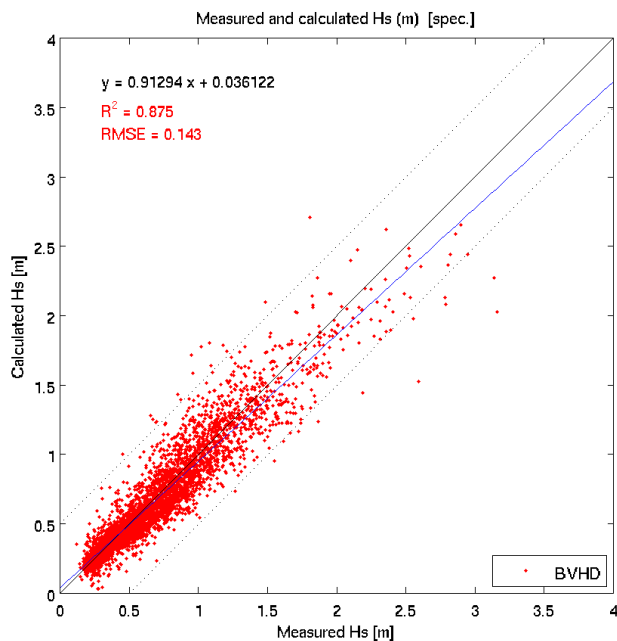


Figure 6-2: Comparison between calculated and measured wave height at Bol van Heist, results of the present SWAN calculations.

## 6.2 Further optimization/calibration

Obtained results show some scatters/errors as can be seen in Figure 6-2. This scatter can be removed if correction factors are introduced for each calculation data. For example the measurement data shows a wave height of 1.0 m at Bol van Heist and the computational result shows a wave height of 1.05 m at Bol van Heist: in this case a correction factor  $1.00/1.05=0.95$  can be used to get same wave height. Figure 6-2 shows the calculated Hs (with correction) against the measured Hs at BVHD. This correction is valid as long as the region of the interest is close to Bol van Heist. As can be seen in Figure 6-3, the region of interest for E1 is close to Bol van Heist. Therefore the correction factors are applied for the nesting for the calculations of the future configuration as a further optimization.

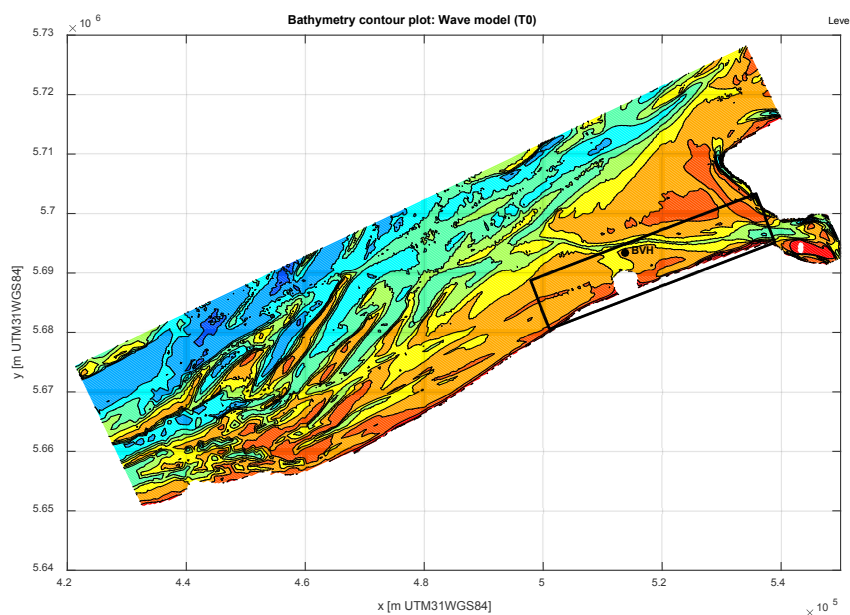


Figure 6-3: Location of Bol van Heist and E1 domain

### 6.3 Output of the model (T0)

In total 3558 cases were calculated for 150 output points between Zeebrugge and the mouth of the Western Scheldt based on a wave climate in 2013 by the T0 model developed in this study. The calculated results are processed using the correction factor explained in the last section. Additionally all the nesting data (full spectrum data) are processed using the same correction factor to be able to use the nesting data for E1 calculation.

Figure 6-4 shows the calculated  $H_s$  (with correction) against the measured  $H_s$  at BVHD, T0. Since it is corrected data, all the relationship became 1:1.

Figure 6-5 shows a comparison between measured and calculated wave heights at Bol van Heist, scenario E1. It can be found in the figure that a few points are outside the trend. The reason is not very clear for this; however it would be better to exclude those extreme points for the further analysis.

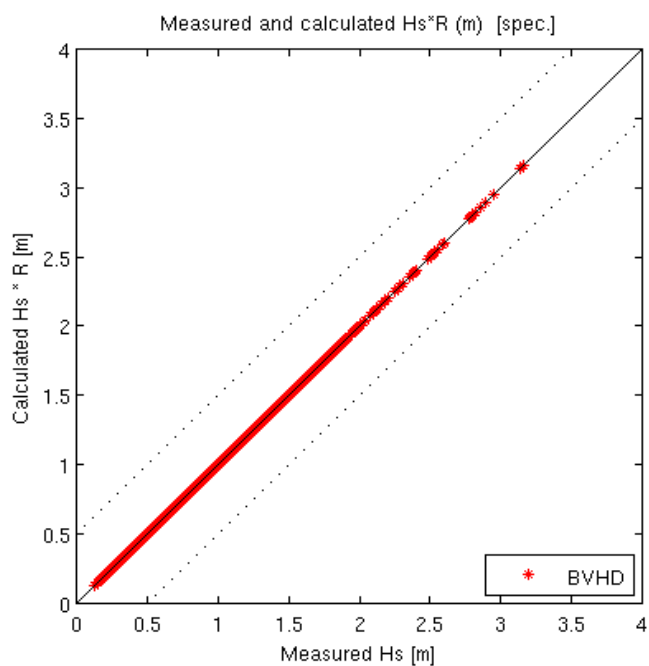
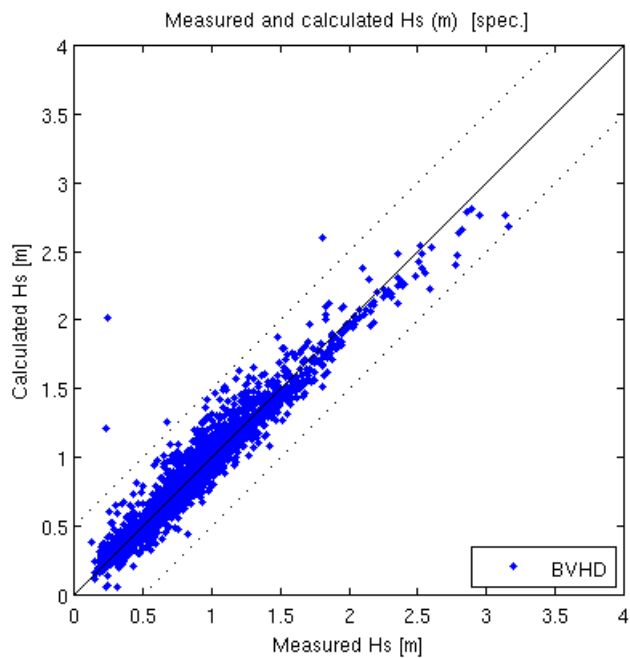


Figure 6-4: Comparison between measured and calculated  $\cdot R$  (correction parameter) wave height at Bol van Heist, T0.



S

Figure 6-5: Comparison between measured and calculated wave heights at Bol van Heist, scenario E1.

## 7 SENSITIVITY ANALYSIS

### 7.1 Introduction

For the future bathymetry calculation (i.e. E1 configuration), some sensitivity analyses are necessary to know which model settings should be applied in the final computation. In Chapter 2 it is concluded that there are some uncertainties for the behavior of diffraction, therefore a sensitivity analysis for grid resolution is necessary. On top of that physical functions in SWAN, namely Triad (wave-wave interaction) and Diffraction have to be tested if they show good behavior in the sensitivity model runs.

### 7.2 Model settings

#### 7.2.1 Bathymetry and domain

A1 configuration is used for this sensitivity analysis. A1 is a relatively simple configuration compared to E1 configuration, so it is easier to judge which settings are the most suitable for calculations with islands.

#### 7.2.2 Grid size and physical processes

The main aim of the sensitivity analysis is to determine the optimal grid size to be used in the model computations in the small study domain (i.e. black box in Figure 6-3). Four different grid sizes were tested with/without extra physical processes in the model. The variety of the grid sizes and physical processes are shown below.

##### Grid size

- 100 x 100 m
- 50 x 50 m
- 20 x 20 m
- 10 x 10 m

##### Physical processes

- Wave-wave interaction, Triad
- Diffraction

#### 7.2.3 Boundary conditions offshore

Boundary conditions at the offshore boundary are set as follows.

- SWL = +2.0 m TAW
- $H_s = 1.0$  m,  $T_p = 4.0$  s (JONSWAP,  $\gamma=3.3$ )
- Wave direction is perpendicular to the coast
- Directional spreading is 30 degree
- No wind

These settings are based on wave height estimation at Knokke in IMDC (2009c), see table below (Table 7-1). A wave height around 1.0 m is not too small for ship navigation and shows a relatively high rate of emergence when the wave period is around 4.0 s. Water level +2.0 m TAW is chosen as an intermediate water level in the tide (generally tide is from around 0 m TAW to 4-5 m TAW).

The wave direction is set as perpendicular to the coast for the simplicity. Directional spreading 30 degree is chosen since 30 degree is used for normal or relatively rough sea state. Wind is not used in this sensitivity analysis for the simplicity.

Table 7-1: Overview of the wave height and period distribution at 5 m TAW at Knokke.

Tabel 5-45 Samengestelde frequentieverdeling van golfhoogte  $H_{m0}$  en golfperiode  $T_{m02}$  op 5m TAW voor de kust van Knokke. (kwantitatief)

	---	<3s	3-4s	4-5s	5-6s	6-7s	>7s	Totaal
<50	2,28%	25,41%	21,39%	9,61%	1,90%	0,45%	0,19%	61,23%
50-75		1,29%	14,04%	1,39%	0,37%	0,02%		17,11%
75-100		0,005%	8,87%	1,02%	0,23%	0,02%		10,15%
100-125			4,50%	1,06%	0,10%	0,04%	0,001%	5,70%
125-150			0,75%	2,06%	0,02%	0,02%	0,002%	2,86%
150-175			0,02%	1,57%	0,02%	0,003%	0,001%	1,61%
175-200				0,72%	0,03%	0,002%	0,003%	0,75%
200-225				0,27%	0,08%	0,001%	0,002%	0,35%
225-250				0,04%	0,12%			0,16%
250-275				0,004%	0,05%			0,05%
275-300					0,01%			0,01%
> 300					0,003%			0,003%

### 7.3 Model results

In this sensitivity analysis 1 boundary condition time's 4 grid resolutions times 2 wave processes, in total 8 cases, have been calculated.

Figure 7-3 shows the computed  $H_s$  [m] with various grid sizes (left: wave processes on, right: off). At first glance each result shows similar wave transformation.

Figure 7-3 shows the difference between the computed  $H_s$  [m] without and with wave processes (diffraction and triad). The difference in wave height is small (i.e. less than 10 cm). On the other hand, looking at Figure 7-3, the wave pattern is somewhat different behind the island. With diffraction and triad the wave pattern is smoother than the one without.

Figure 7-3 shows the difference between different grid sizes (wave processes were switched on). It shows that the difference between 100 m and 10 m or 50 m grid can be big (more than 20 cm). However if we have a closer look at the vicinity of the island where a big difference can be seen (Figure 7-4), there is some gap around the edge of the islands. This gap is made due to the interpolation process when the bathymetry is made. This creates a big difference in wave height. Actually the difference in diffraction is not too big if looking at the other side of the island where there is no gap in bathymetry. Therefore this difference can be avoided if the bathymetry is made with care (i.e. no gap in island bathymetry).

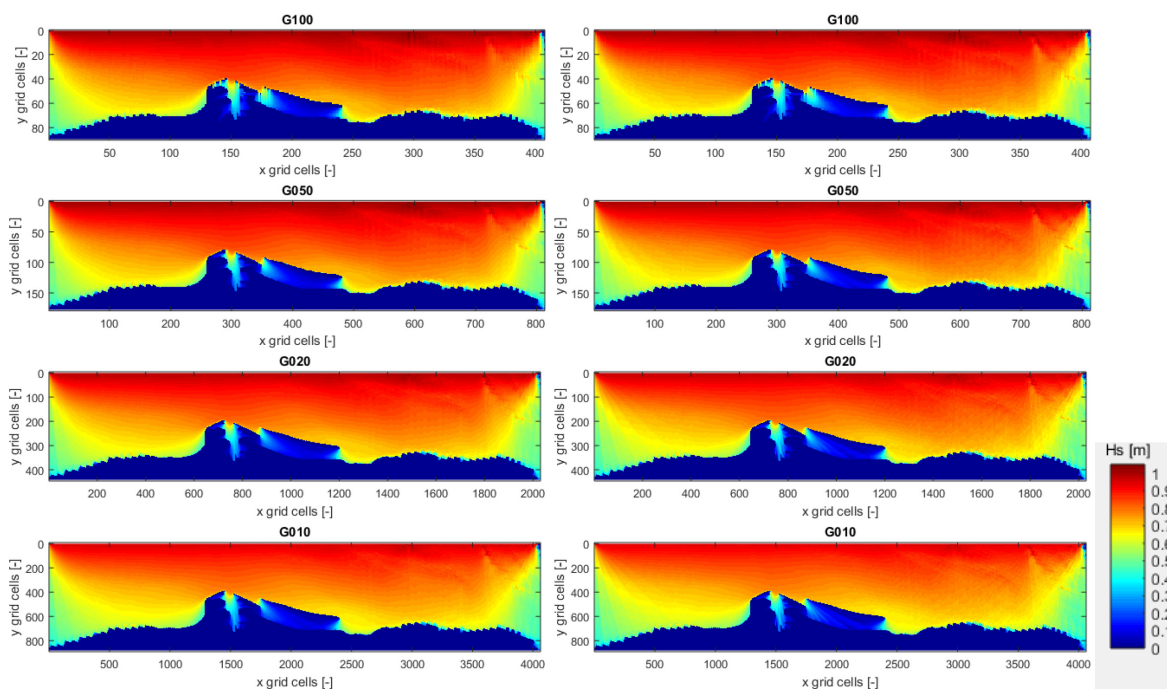


Figure 7-1: Computed  $H_s$  [m] with various grid sizes (left: wave processes on, right: off) for configuration A1.

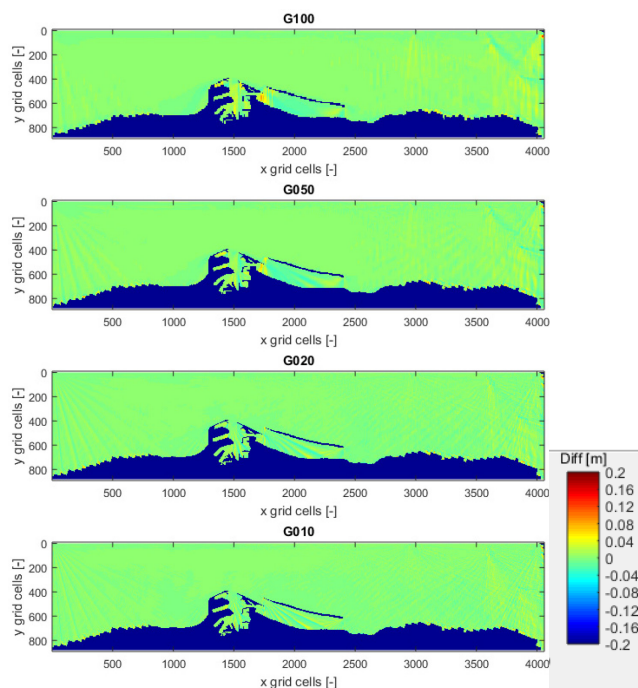


Figure 7-2:  $H_s$  difference between wave processes on and off.



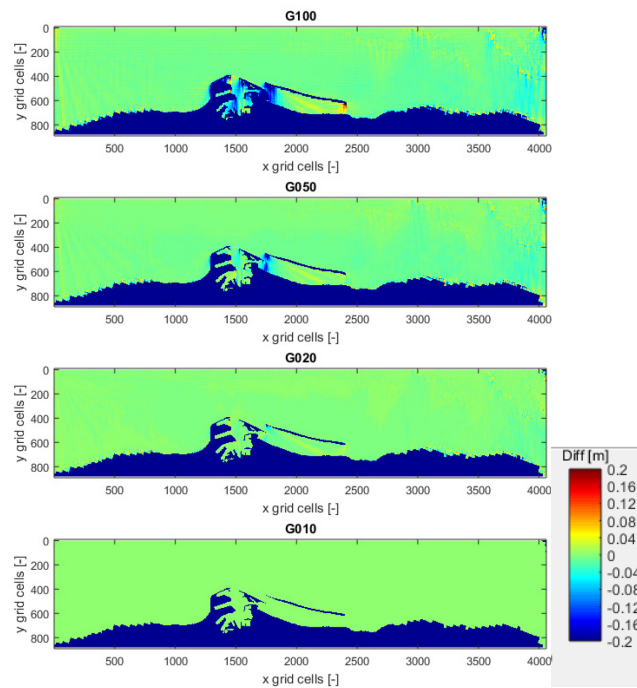


Figure 7-3: Hs difference between 10 m grid and each grid.

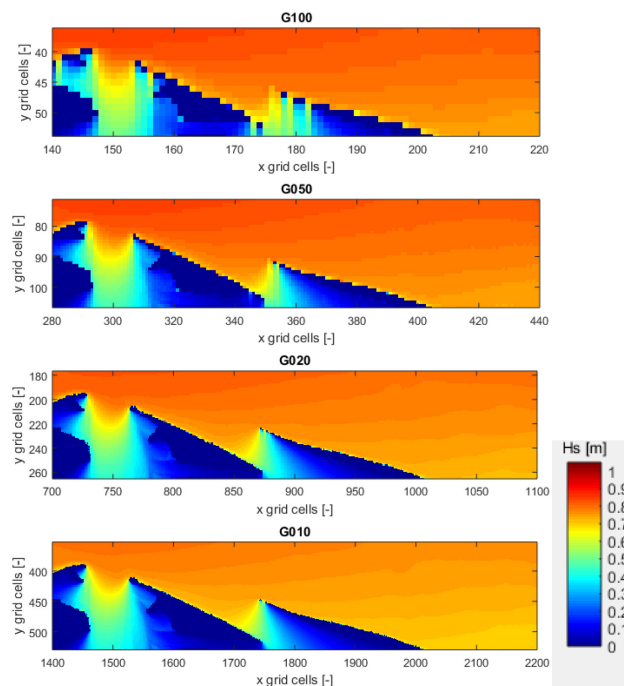


Figure 7-4: Closer view on the tip of the island

## 7.4 Computational cost

The computational cost for 1 year calculations (~4000 runs) by one node consisting of 12 cores in the cluster in WL is shown below.

- 100 x 100 m: less than 1 day
- 50 x 50 m: around 4 days
- 20 x 20 m: around 25 days
- 10 x 10 m: around 100 days

## 7.5 Conclusions

Based on the model results and computational cost, we decided to use a 50 x 50 m grid for the E1 configuration. Even though there are some differences in wave height around the tip of the island due to the bathymetry. It is believed that this can be avoided if the bathymetry is made with caution. This decision of choosing 50 x 50 m grid is a good compromise between quality of the result and computational cost.

## 8 SIMULATION RESULTS FOR CONFIGURATION E1

### 8.1 Bathymetry of E1

As pointed out in the sensitivity analysis, generating the bathymetry is a very important issue. For E1, special care is taken when the bathymetry was made. Using a criterion of +1 m TAW (above this level we set NaN, Not a Number value shown by white color where calculation is skipped) for the interpolation process, the islands became continuous (there is no gap).

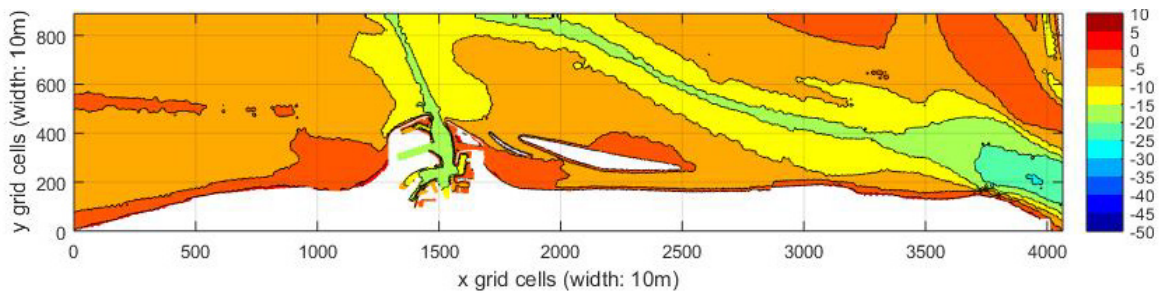


Figure 8-1: Bathymetry contour plot as used in SWAN model computation of scenario E1.

### 8.2 Validity of E1 model

Figure 8-2 shows one example of the calculation of T0 and E1 (id number=4280; 23/12/2013 16:00:00) to illustrate how nesting works. As can be seen in the figure, the nesting is working well: the wave height is comparable with each other. Behind the island the wave height is different due to shading effect of islands.

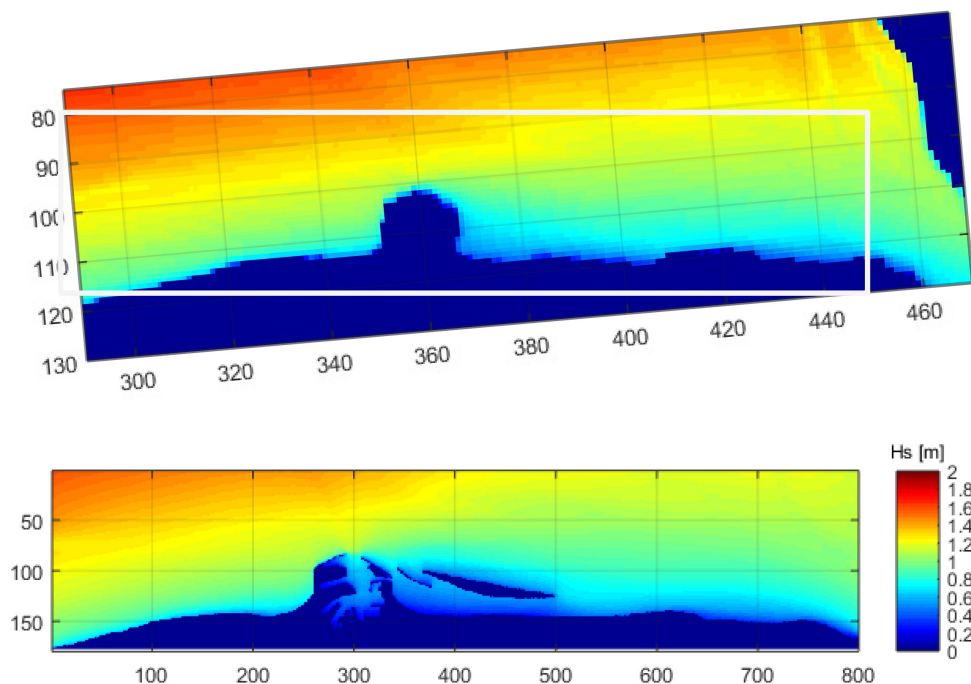


Figure 8-2: Comparison of Hs between T0 (top panel) and E1 (bottom panel).

### 8.3 Output of the model calculations for E1

In total 3368 cases were calculated for 150 output points between Zeebrugge and the mouth of the Western Scheldt based on a wave climate in 2013 by the E1 model developed in this study. Some strange behavior in terms of wave height can be seen in the output (e.g. all the result of  $H_s$  is zero), so those are excluded for the final result (190 cases). As a result in total for 3368 cases calculations were performed and output was generated.

### 8.4 Example of spatial output for shading effect (E1)

Even though analysis of the calculated wave data is not the purpose of this report, some calculated examples are shown here.

In this section, an example of the shadow effect by the new islands in the E1 configuration is investigated by comparing 4 different wave directions NNW, NW, WNW, W. Wave direction NNW, - 22.5 degree to the north, is almost perpendicular to the coastal line since the rotation of E1 from the left down corner is 21.04 degree.

Figure 8-3 shows the wave height ratio (= local significant wave height / wave height at BVH) for each wave directions. We have selected cases which wave height is around 1.0 m at BVH and wind is calm ( $u$  is less than 5m/s, see each figure), to be able to compare the shadow effects for different direction under similar conditions. Behind the islands the ratio is between 0.1-0.3. Difference by the wave direction in terms of shading effect is very limited as long as this figure is concern.

Figure 8-4 shows the wave height ratio for the specific wave direction NNW. In this case we selected the cases in which wave height is around 1.0 m at BVH with relatively big East wind (more than 5m/s). In this case behind the islands the ratio is between 0.4-0.5. This is due to the influence of wind speed and direction (east wind can generate waves behind the islands). Note that this ratio change will depend on the significant wave height at BVH: when wave height is big e.g. 3.0 m, even strong East wind does not influence too much to the ratio since absolute value behind the island is bigger. On the other hand, when the wave height at BVH is smaller than e.g. 0.5 m, then wind effect can dominate the area behind the islands.

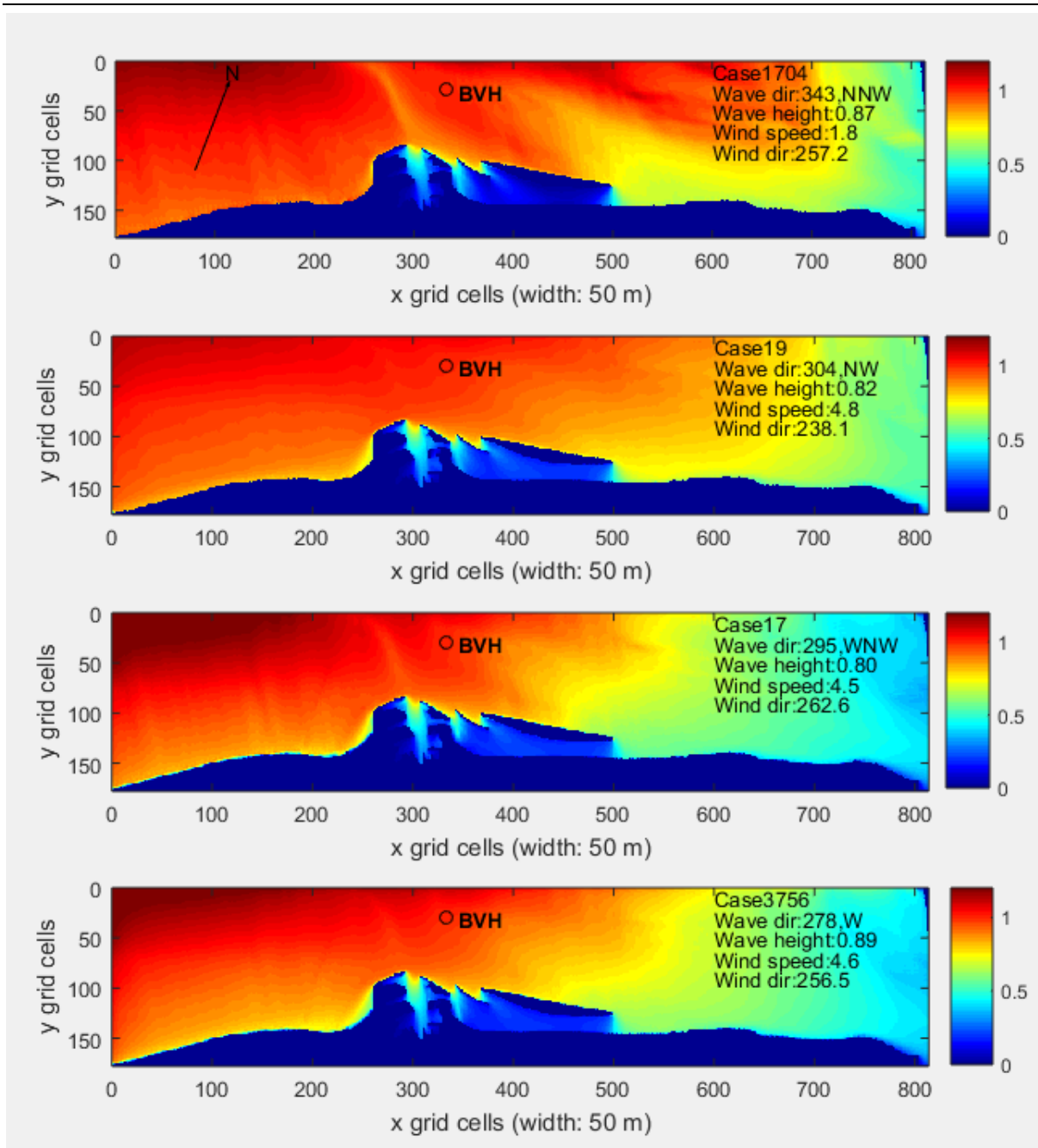


Figure 8-3: Wave shading effect by the new islands (wave dir.: NNW, NW, WNW, W)

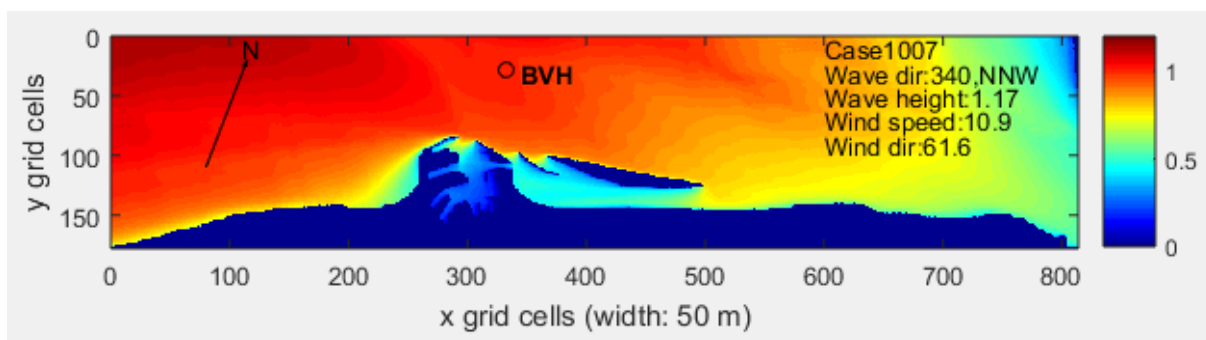


Figure 8-4: Wave shading effect by the new islands (wave dir.: NNW) combined with strong E wind

## 9 CONCLUSIONS

In this study, the Belgian coast model in SWAN has been applied to estimate the wave climate between Zeebrugge and the mouth of the Western Scheldt at present and possible future situations. The wind and hydraulic boundary conditions of the year 2013 have been applied in this study to estimate the wave climate in the study area. The model computations are focusing mainly on two different scenarios. T0 scenario represents the existing situation and Scenario E1 with future recommended islands. The settings of the model for the future scenario E1 has been selected based on the outcomes/lesson learned from series of previous studies (e.g. Verwaest et al. 2008; IMDC 2005; 2006; 2008; 2009a; 2009b; 2009c), and also on the sensitivity analyses performed in this study with configuration A1.

The model results are.

- T0 wave climate (3558 cases calculated for 150 output points between the port of Zeebrugge and the mouth of the Western Scheldt);
- E1 wave climate (3368 cases calculated for 150 output points between the port of Zeebrugge and the mouth of the Western Scheldt).

Data can be used for the further analysis of ship navigation in the study area.

## 10 REFERENCES

- AMT (2014): Masterplan Vlaamse Baaien, 75pp, Afdeling Maritieme Toegang, Departement MOW, Vlaamse Overheid. <http://mow.vlaanderen.be/vlaamsebaaien/masterplan.pdf>
- Booij, N., Holthuijsen, L.H., and P.H.M. de Lange, 1993. The penetration of short-crested waves through a gap, Proc. 23rd Int. Conf. Coastal Eng, Venice 4-9 Oct., 1992, New York, 1993, 1044-1052.
- Boshek M., 2009. Reflection and diffraction around breakwaters. Master of Science Thesis, Faculty of Civil Engineering and Geosciences, TU Delft, The Netherlands.
- De Roo, S.; Trouw, K.; Ruiz Parrado, I.; Willems, P.; Suzuki, T.; Verwaest, T.; Mostaert, F. (2015). Het Hydraulisch Randvoorwaardenboek 2014: Achtergrondrapport. Versie 2.0. WL Rapporten, 14\_014. Waterbouwkundig Laboratorium & Fides Engineering: Antwerpen, België.
- Enet, F., Nahon, A., Vledder, G. Van, & Hurdle, D. (2006). Evaluation of diffraction behind a semi-infinite breakwater in the SWAN Wave Model. Symposium on Ocean Wave, 1–14. Retrieved from <ftp://www.wmo.int/Documents/PublicWeb/amp/mmop/documents/JCOMM-TR/J-TR-34-9th-waves-workshop/Papers/Enet.pdf>
- Holthuijsen, L.H., Herman, A. and Booij, N., 2003. Phase-decoupled refraction-diffraction for spectral wave models, Coastal Engineering, 49, 291-305.
- IMDC (2005), Afstemming Vlaamse en Nederlandse voorspelling golfklimaat op ondiep water – Deelopdracht 1: Voorbereiding tijdreeksen met randvoorwaarden in opdracht van WLH.
- IMDC (2006), Afstemming Vlaamse en Nederlandse voorspelling golfklimaat op ondiep water – Deelopdracht 2: Voortzetting validatie numeriek model in opdracht van WLH.
- IMDC (2008), Afstemming Vlaamse en Nederlandse voorspelling golfklimaat op ondiep water – Deelopdracht 4: Technisch Wetenschappelijke bijstand – Traject Golfklimaat.
- IMDC (2009a), Afstemming Vlaamse en Nederlandse voorspelling golfklimaat op ondiep water – Deelopdracht 4: Technisch Wetenschappelijke bijstand – Eindrapport.
- IMDC (2009b), Afstemming Vlaamse en Nederlandse voorspelling golfklimaat op ondiep water – Deelopdracht 4: Technisch Wetenschappelijke bijstand – Traject Onderzoek.
- IMDC (2009c), Afstemming Vlaamse en Nederlandse voorspelling golfklimaat op ondiep water – Deelopdracht 5: Rapportage jaargemiddelde golfklimaat.
- KULeuven/WLH (2004), Opmaak van een numerieke golfdatabank voor de Vlaamse kust.
- Lin J-G. 2013. An improvement of wave refraction-diffraction effect in SWAN, J. Marine Sci. Tech., 21(2), 198-208.
- Rusu, E., Pilar, P., and Guedes Soares, C., 2008. Evaluation of the wave conditions in Madeira Archipelago with spectral models. Ocean Engineering, 35, 1357–1371.
- The SWAN team, 2015. SWAN scientific and technical documentation, Cycle III, version 41.01A, Delft University of Technology, Delft, The Netherlands.
- Vantorre, M.; Eloot, K.; Geerts, S. (2013). Inland vessels at sea: a useful contradiction to solve missing links in waterway systems, in: Rigo, P. et al. (Ed.) (2013). PIANC - SMART Rivers Conference 2013, 23 - 27 September 2013 - Maastricht / Liège: Proceedings. pp. paper 25 [1-9],
- Verwaest, T., Doorme, S., Verelst, K., and Trouw, K. (2008). The wave climate in the Belgian coastal zone, Proceedings 9th International Conference LITTORAL 2008. A Changing Coast: Challenge for the Environmental Policies, Venice, Italy.

## 11 APPENDIX A

Location of the output locations (out4, total 150 points) in x and y coordinate in WGS84UTM31.

x,y [m in UTM31WGS84]	x,y [m in UTM31WGS84]	x,y [m in UTM31WGS84]
526388.6135,5692150.4171	526146.4613,5693010.5556	526261.6455,5705086.4051
526388.6135,5692150.4171	524166.5390,5692392.7474	528592.2515,5705990.9910
525720.1993,5693445.6417	522186.6601,5691773.9420	530922.8575,5706895.5769
546793.2535,5692066.5825	520206.7593,5691156.1373	533253.4635,5707800.1628
546836.9931,5691676.9662	518226.8692,5690538.3342	497084.4341,5690921.6046
546836.9931,5691676.9662	516246.9897,5689920.5326	499411.5202,5691835.2076
521007.1822,5694659.5238	515752.0133,5689766.3322	501738.6062,5692748.8107
503343.0606,5693572.3345	536046.2377,5696099.6262	504065.6922,5693662.4138
528643.4391,5697418.5737	534071.9137,5695308.9771	506392.7783,5694576.0169
513823.1367,5693152.3600	532097.6009,5694518.3322	508719.8643,5695489.6200
513367.1805,5690247.3235	530123.3320,5693726.6922	511046.9503,5696403.2230
514253.8017,5691207.3722	528149.0416,5692936.0551	513374.0364,5697316.8261
536203.0850,5696104.7568	526174.7622,5692145.4218	515701.1224,5698230.4292
515554.2167,5689759.8607	524200.4938,5691354.7922	518028.2085,5699144.0323
536046.2377,5696099.6262	522226.2691,5690563.1672	520355.2945,5700057.6353
534060.6067,5695654.6386	520252.0227,5689772.5447	522682.3805,5700971.2384
532074.9867,5695209.6514	518277.7871,5688981.9256	525009.4666,5701884.8415
530089.3775,5694764.6644	516303.5624,5688191.3097	527336.5526,5702798.4446
528103.7791,5694319.6777	515810.0242,5687993.1567	529663.6386,5703712.0477
526118.1914,5693874.6911	495963.7674,5693326.7885	531990.7247,5704625.6507
524132.5816,5693430.7036	498294.3734,5694231.3744	534525.8949,5705620.9467
522147.0149,5692985.7172	500624.9794,5695135.9603	498140.2918,5688655.5144
520161.4588,5692540.7307	502955.5854,5696040.5462	500467.4853,5689568.8437
518175.9130,5692095.7441	505286.1914,5696945.1321	502794.6788,5690482.1730
516190.3775,5691650.7574	507616.7974,5697849.7180	505121.8723,5691395.5022
515693.9952,5691539.5107	509947.4034,5698754.3039	507449.0658,5692308.8315
514204.8521,5691205.7705	512278.0094,5699658.8898	509776.2593,5693222.1608
536046.2377,5696099.6262	514608.6154,5700563.4757	512103.4529,5694135.4901
534066.2603,5695481.8079	516939.2214,5701468.0615	514430.6464,5695048.8194
532086.2940,5694863.9917	519269.8274,5702372.6474	516757.8399,5695962.1486
530106.3388,5694246.1777	521600.4335,5703277.2333	519085.0334,5696875.4779
528126.3946,5693628.3657	523931.0395,5704181.8192	521412.2269,5697788.8072
(32 points)	(32 points)	(32 points)



Wave climate for inland vessels between Zeebrugge and the mouth of the Western Scheldt:  
 Estimation by the Belgian coast model in SWAN

---

x,y [m in UTM31WGS84]	x,y [m in UTM31WGS84]	
523739.4204,5698702.1365	521198.7021,5692338.3187	
526066.6139,5699615.4658	523526.1126,5693251.0947	
528393.8074,5700528.7950	525853.5232,5694163.8708	
530721.0009,5701442.1243	528180.9337,5695076.6468	
533048.1944,5702355.4536	530508.3443,5695989.4229	
535457.4760,5703300.9991	532835.7548,5696902.1990	
499196.1495,5686389.4243	535163.1654,5697814.9750	
501523.4512,5687302.4779	537320.6381,5698661.1040	
503850.7528,5688215.5315	517549.0000,5690300.0000	
506178.0545,5689128.5851	518849.0000,5690390.0000	
508505.3562,5690041.6387	520155.0000,5690560.0000	
510832.6579,5690954.6923	521382.0000,5690780.0000	
513159.9595,5691867.7459	522708.0000,5691030.0000	
515487.2612,5692780.7996	515997.0429,5689846.5316	
517814.5629,5693693.8532	517452.2541,5689714.2396	
520141.8646,5694606.9068	518857.8559,5689912.6775	
522469.1662,5695519.9604	520079.9026,5690210.3344	
524796.4679,5696433.0140	521201.0767,5690574.1372	
527123.7696,5697346.0676	522242.8757,5690971.0130	
529451.0713,5698259.1212	523284.6746,5691301.7428	
531778.3730,5699172.1749	524227.2547,5691715.1551	
534105.6746,5700085.2285	514387.1790,5691918.7920	
536389.0570,5700981.0516	(22 points)	
500252.0071,5684123.3341		
502579.4177,5685036.1102		
504906.8282,5685948.8862		
507234.2388,5686861.6623		
509561.6493,5687774.4384		
511889.0599,5688687.2144		
514216.4704,5689599.9905		
516543.8810,5690512.7665		
518871.2915,5691425.5426		
(32 points)		

## 12 APPENDIX B

Input example for SWAN run (T0)

Input SWAN file [GT0\_test\_0001.swn]

---

```
-----
$*****HEADING*****
$
PROJ 'GT0_test_0001' '01'
$
$*****MODEL INPUT*****
$
SET LEVEL 4.18
SET NAUT
MODE STATIONARY
MODE TWOD
$
CGRID REG      438116  5639190  25.50  125000  39000  500  156  CIRCLE 36 0.025 0.85 37
$
INPGRID BOTTOM  438116  5639190  25.50   500   156  250  250  EXC -999
$
READINP BOTTOM 1.0 'wgs84_taw_swan.dep' 4 0 FREE
$
BOU SIDE N CCW      CON FILE 'GT0_test_0001.bn1' 1
BOU SEGM IJ 500 80 500 156 CON FILE 'GT0_test_0001.bn2' 1
BOU SIDE W CCW      CON FILE 'GT0_test_0001.bn3' 1
$
GEN3 WESTHUYSEN
BREAK CON 1.00 0.73
FRIC JON 0.067
WIND 11.1 200.7
$
NUM STOPC STAT 50
$
$***** OUTPUT *****
$
OUTPUT OPTIONS TABLE 16 BLOCK 9 6
$
POINTS 'WHID' 461245.189 5692631.670
TABLE 'WHID' HEAD 'GT0_test_0001_WHID.tab' XP YP DEP HS RTP DIR TM01 TM02 WIND TMM10
SPEC 'WHID' SPEC1D ABS 'GT0_test_0001_WHID.sp1'
SPEC 'WHID' SPEC2D ABS 'GT0_test_0001_WHID.sp2'
POINTS 'AKZD' 487386.200 5696115.280
TABLE 'AKZD' HEAD 'GT0_test_0001_AKZD.tab' XP YP DEP HS RTP DIR TM01 TM02 WIND TMM10
SPEC 'AKZD' SPEC1D ABS 'GT0_test_0001_AKZD.sp1'
SPEC 'AKZD' SPEC2D ABS 'GT0_test_0001_AKZD.sp2'
POINTS 'BVHD' 514387.179 5691918.792
TABLE 'BVHD' HEAD 'GT0_test_0001_BVHD.tab' XP YP DEP HS RTP DIR TM01 TM02 WIND TMM10
SPEC 'BVHD' SPEC1D ABS 'GT0_test_0001_BVHD.sp1'
SPEC 'BVHD' SPEC2D ABS 'GT0_test_0001_BVHD.sp2'
```

```
POINTS 'out4' FILE 'out4.txt'
TABLE 'out4' HEAD 'GTO_test_0001_out4.tab' XP YP DEP HS RTP DIR TM01 TM02 WIND TMM10
SPEC 'out4' SPEC1D ABS 'GTO_test_0001_out4.sp1'
SPEC 'ou4' SPEC2D ABS 'GTO_test_0001_out4.sp2'
BLOCK 'COMPGRID' NOHEAD 'GTO_test_0001_xp.mat' LAY-OUT 1 XP
BLOCK 'COMPGRID' NOHEAD 'GTO_test_0001_yp.mat' LAY-OUT 1 YP
BLOCK 'COMPGRID' NOHEAD 'GTO_test_0001_dep.mat' LAY-OUT 1 DEP
BLOCK 'COMPGRID' NOHEAD 'GTO_test_0001_hs.mat' LAY-OUT 1 HS
BLOCK 'COMPGRID' NOHEAD 'GTO_test_0001_tmm10.mat' LAY-OUT 1 TMM10
BLOCK 'COMPGRID' NOHEAD 'GTO_test_0001_per.mat' LAY-OUT 1 PER
BLOCK 'COMPGRID' NOHEAD 'GTO_test_0001_rtp.mat' LAY-OUT 1 RTP
BLOCK 'COMPGRID' NOHEAD 'GTO_test_0001_tps.mat' LAY-OUT 1 TPS
BLOCK 'COMPGRID' NOHEAD 'GTO_test_0001_dspr.mat' LAY-OUT 1 DSPR
BLOCK 'COMPGRID' NOHEAD 'GTO_test_0001_dir.mat' LAY-OUT 1 DIR
BLOCK 'COMPGRID' NOHEAD 'GTO_test_0001_pdir.mat' LAY-OUT 1 PDIR
BLOCK 'COMPGRID' NOHEAD 'GTO_test_0001_ubot.mat' LAY-OUT 1 UBOT
BLOCK 'COMPGRID' NOHEAD 'GTO_test_0001_urms.mat' LAY-OUT 1 URMS
BLOCK 'COMPGRID' NOHEAD 'GTO_test_0001_dhsign.mat' LAY-OUT 1 DHSIGN
BLOCK 'COMPGRID' NOHEAD 'GTO_test_0001_drtm01.mat' LAY-OUT 1 DRTM01
$
COMPUTE
STOP
$
```

-----  
-----

DEPARTMENT **MOBILITY & PUBLIC WORKS**  
Flanders hydraulics Research

Berchemlei 115, 2140 Antwerp

T +32 (0)3 224 60 35

F +32 (0)3 224 60 36

[waterbouwkundiglabo@vlaanderen.be](mailto:waterbouwkundiglabo@vlaanderen.be)

[www.flandershydraulicsresearch.be](http://www.flandershydraulicsresearch.be)